ISSN: 2359-1048
Novembro 2021

A spatio-temporal approach to estimate changes in the patterns of fire occurrence in the Legal Amazon

FERNANDA VALENTE
FEA-RP/USP - FACULDADE DE ECONOMIA, ADMINISTRAÇÃO E CONTABILIDADE DE RIBEIRÃO PRETO DA USP

MÁRCIO POLETTI LAURINI
UNIVERSIDADE DE SÃO PAULO - USP

Introdução
The Amazon biome plays an important role in the climate system, with relevance at regional and global scales. Fire occurrences, related to both natural and anthropogenic activities, are relevant disturbances in the Legal Amazon, with significant effects. Changes in the patterns of fire occurrence in the Amazon region have been widely reported in the literature and are related with a variety of factors, including dry conditions, deforestation, agricultural expansion, climate changes, and climatic anomalies such as El Ninõ events.

Problema de Pesquisa e Objetivo
The purpose of this paper is to analyze the existence of changes in the patterns of the fire occurrence in the Legal Amazon, within the spatio-temporal point process framework. To do this, we propose a novel methodology to extent the trend-cycle decomposition in spatio-temporal models to spatio-temporal point pattern data, by proposing to use a dynamic representation of a Log Gaussian Cox process (LGCP) where the intensity function is modeled through the decomposition of components into trend, seasonality, cycles, covariates and spatial effects.

Fundamentação Teórica
The LGCP is a particular case of the Cox process, where the log-intensity function is a Gaussian field. Due to the stochastic property of the LGCP, fitting this model is often computationally expensive. In this sense, to perform the estimation in a computationally effective way, we use the stochastic partial differential equation approach to transform the initial Gaussian field to a Gaussian Markov Random Field, which is defined by sparse matrices. Furthermore, the resulting Bayesian hierarchical model fits within the integrated nested Laplace approximations framework (Rue et al., 2009).

Metodologia
To perform inference procedures, we proposed a structural decomposition to spatio-temporal point pattern data. In particular, we proposed to use a dynamic representation of a Log Gaussian Cox process where the intensity function was modeled through the decomposition of components into trend, seasonality, cycles, covariates and spatial effects. This useful formulation was able to capture permanent changes in the fire occurrence and also, to identify seasonal and cyclic effects (Laurini, 2019; Valente e Laurini, 2020).

Análise dos Resultados
The results show that long-term movements of fire activity dropped considerably between 2006 and 2012, which suggest that conservation regulations and/or market conditions in the mid-2000s were effective in reducing the fire events. Also, our model captured an increase in the trend component between 2013 and 2016, and after 2018, which may be explained by localized drivers associated with political measures that encourage the expansion of agriculture and livestock.

Conclusão
The estimated components suggested relevant changes in the patterns of the fire activity in the Legal Amazon. In particular, it is possible to observe how the long-term component is affected by conservation regulations and/or market conditions, i.e., the obtained evidences suggest that the changes in the fire ocorrences are mostly related to human-induced activities. Furthermore, the seasonal component provided evidence that fire events in the Legal Amazon has become more consistent throughout the year, suggesting the increase of fuel management practices occurring during the nonfire season.

Referências Bibliográficas
Laurini, M., 2019. A spatio-temporal approach to estimate patterns of climate change. Environmetrics 30, e2542. Valente, F., Laurini, M., 2020. Tornado occurrences in the united states: A spatio-temporal point process approach. Econometrics8, 25. Rue, H., Martino, S., Chopin, N., 2009. Approximate bayesian inference for latent Gaussian models by using integrated nestedLaplace approximations. Journal of the Royal Statistical Society: Series B (Statistical Methodology) 71, 319–392.

Palavras Chave
Legal Amazon, Fire Occurrence, Spatio-temporal models

Agradecimento a orgão de fomento
The authors acknowledge funding from CNPq (306023/2018-0), FAPESP (2018/04654-9), Coordenação de Aperfeiçoamento de Pessoal de Nível Superior (CAPES) - Finance Code 001 and Instituto Escolhas.

A SPATIO-TEMPORAL APPROACH TO ESTIMATE CHANGES IN THE PATTERNS OF FIRE OCCURRENCE IN THE LEGAL AMAZON

1. Introduction. The Amazon biome is one of Earth's greatest biological treasures, containing more than half of the world's rainforests and a quarter of all terrestrial species (Malhi et al., 2008). The Amazon rainforest also provides an environmental service by storing carbon, in both biomass and soils, and thus reducing the global warming (Fearnside, 2012). Plus, evaporation and precipitation over Amazonia play an important role in the global atmospheric circulation, with effects on the climate across South America and North Hemisphere (Gedney and Valdes, 2000; Werth and Avissar, 2002). Although the Amazon rainforest is shared by nine countries, about 60 percent of the Amazon Basin is in Brazil, where the political-administrative area called Legal Amazon encompasses nine Brazilian states, corresponding to 61% of the national territory.

Fire occurrences, related to both natural and anthropogenic activity, are relevant disturbances in the Amazon region, affecting the atmosphere composition (Crutzen and Andreae, 1990; Longo et al., 2009), forest structure and composition (Cochrane and Schulze, 1999), and the cycle of carbon. In general, fire occurrence in the Amazon rainforest is related to land use, land cover, and climate patterns. In terms of total forest loss and fire occurrence, most of the changes in the land cover and human activities are concentrated along with the southern and eastern extent of the Brazilian Amazon region, called "arc of deforestation" (Morton et al., 2006), which is related to the presence of roads and human accessibility (Siegert et al., 2001; Serra et al., 2014). The expansion of roads and agriculture in the Legal Amazon began in the early 1970s when the Transamazon Highway was built. The construction of roads was accompanied by high rates of deforestation. For instance, between 1980 and 1990, the rates of deforestation in the Legal Amazon increased considerably, where approximately 225000km^2 of forest were cleared. In the same period, the extension of paved roads increased by more than 100% and unpaved roads increased by approximately 460% (Ferraz, 2001).

From an economic standpoint, the fire occurrence in the Amazon region generates a great variety of costs with private and social consequences. In rural properties, the main losses occur when burning gets out of control and spread into pasture and forest areas. Also, losses related to fire occurrence may reach social proportions, through the release of carbon into the atmosphere, affecting global climate patterns, and provoking adverse health outcomes which impose direct and indirect costs on society, such as medical costs, labor loss, and utility loss De Mendonça et al. (2004, 2006).

Many factors may change the patterns of fire occurrence in the Amazon region. Previous studies have reported the impact of dry conditions on forest fire risk (Nepstad et al., 2004; Aragão et al., 2007), and the effects of deforestation and fragmentation on regional climate, which have shown a significant increase in the mean surface temperature, and a decrease in the annual evapotranspiration and precipitation, which can further increase fire danger (Nobre et al., 1991; Costa et al., 2007). Changes in the patterns of forest fire has also been reported to be related to agricultural expansion (Morton et al., 2008), as agriculture is the main driver of deforestation and forest degradation (Food and of The United Nations, 2020), and the fire is a common and inexpensive tool used by Brazilian farmers to expand agricultural frontiers and to maintain and renew pastures. Also, due to climatic change, circulation shifts and increased anomalies such as El Niño events exacerbate extreme dry seasons in Amazonia (Marengo, 2004; Li et al., 2006; Marengo et al., 2008), changing the vegetation structure, potentially transforming the forest from highly resistant to fire ignition to extensively flammable (Cochrane and Barber, 2009), eventually leading to future increases burning frequency. Furthermore, there is evidence that forest fires create positive feedbacks in fire susceptibility, fuel loading, and fire intensity whereby recurrent fires become more likely and severe (Cochrane et al., 1999; Siegert et al., 2001).

One way to verify the existence of changes in the patterns of the climate-related events, such as fire occurrence, is through the estimation of permanent and periodic components (Bloomfield, 1992; Proietti and Hillebrand, 2017; Laurini, 2019), using statistical tools to decompose the observed temporal variability

into trend, seasonal and cycle components. However, the existing methods used to extract trends, seasonal, and cycle components face some problems to perform inference procedures on climate-related issues. First, these models are not fully adapted to the dimensionality of data sources used in climatology. Also, it does not take into account the spatial heterogeneity of climate effects. An alternative way to circumvent the aforementioned problems is a method that combines elements of structural time series decomposition with spatio-temporal models with continuous spatial random effects, which can be thought as a process of decomposing geostatistical time series into a sum of trend, seasonal and cycle components and the effect of additional covariates Laurini (2019); Valente and Laurini (2020).

The purpose of this paper is to analyze the existence of changes in the patterns of the fire occurrence in the Legal Amazon, within the spatio-temporal point process framework. To do this, we propose a novel methodology to extent the trend-cycle decomposition in spatio-temporal models to spatio-temporal point pattern data, by proposing to use a dynamic representation of a Log Gaussian Cox process (LGCP) where the intensity function is modeled through the decomposition of components into trend, seasonality, cycles, covariates and spatial effects (Laurini, 2019; Valente and Laurini, 2020). This is a useful formulation to identify possible changes in the intensity of occurrence over time, such as permanent changes in the fire occurrence, and to capture seasonal and cyclical effects.

The LGCP is a particular case of the Cox process, where the log-intensity function is a Gaussian random field. Due to the stochastic property of the LGCP, fitting this model is often computationally expensive. In this sense, to perform the estimation in a computationally effective way, we use the stochastic partial differential equation (SPDE) approach (Lindgren et al., 2011) to transform the initial Gaussian random field (GRF) to a Gaussian Markov Random Field (GMRF), which is defined by sparse matrices. Furthermore, the resulting Bayesian hierarchical model fits within the integrated nested Laplace approximations (INLA) framework (Rue et al., 2009), also providing significant computational improvements.

We present here, the results of analyzing data for fire occurrence in the Legal Amazon, from January 2003 to February 2020. Our database contains daily fire reports from Moderate-Resolution Imaging Spectroradiometer (MODIS), with information such as spatial coordinates and temporal instant of fire events. Also, we include explanatory variables to control the main fixed effect related to climatic conditions and the use of the soil in agricultural activities. Our results show that long-term movements of fire occurrence dropped considerably between 2006 and 2012, which suggest that conservation regulations and/or market conditions in the mid-2000s were effective in reducing the deforestation rates and, consequently, decreasing the fire occurrence. Also, the reversal of the deforestation decline observed between 2006 and 2012 was capture by our model, showing an increase in the long-term behavior between 2013 and 2016, which may be explained by market mechanisms, and localized drivers such as population growth, investments, and roads, associated with reducing restrictions of Brazil's Forest Code. Also, the deforestation surge in 2016 was accompanied by the political uncertainty surrounding the president Dilma Rousseff's official impeachment proceeding, which offered opportunities to approve legislative initiatives to remove environmental restrictions. Furthermore, our model was able to capture an increase in the trend component after 2018, which may be linked to recent Brazilian political change. Furthermore, the estimated seasonal component provided evidence that fire occurrence in the Legal Amazon has become more consistent throughout the year, suggesting the increase of fuel management practices occurring during the nonfire season, which is related to the expansion of agricultural production.

Our paper proceeds as follows. In section 2 we present the proposed method. Section 3 presents our data. In section 4 we present the results. We conclude in Section 5

2. Methods. Among models for the spatial point process, the Poisson process is the most fundamental structure. However, its application is limited due to its simplistic nature (Teng et al., 2017), even if one assumes a non-homogeneous distribution in space through a function of deterministic intensity. The limitations are related to the lack of possible sources of uncertainty and the fact that the Poisson process is conditionally independent. A related, but more flexible structure, is the Log Gaussian Cox process, a hierarchical structure where at the first level the process is assumed Poisson conditional on the intensity function, and at the second level, the log of the intensity function is assumed to be a Gaussian field (Teng et al., 2017).

Given the doubly-stochastic property of the LGCP, fitting this model is a computational challenge. Within the Bayesian framework, the conditional autoregressive approach is a possible alternative to perform inference procedure and may be fitted using the INLA (Illian et al., 2010). However, this approach is based on regular lattices over the observation window (Simpson et al., 2016), which could be highly inefficient since it requires to construct a much fine grid. For spatial models that combine a GRF with a Matérn correlation structure, the stochastic partial differential equations approach is a way to bypass the problem of inefficiency in the estimation under INLA method. The key of the approach is to use the fact that a GRF with Matérn covariance function is a solution to a SPDE and then the SPDE representation is used in conjunction with basis representation to construct a discrete approximation of the continuous field over the vertices of a 2-dimensional mesh covering the spatial domain (Simpson et al., 2016), i.e., the idea of the SPDE approach is to approximate the initial Gaussian field to a Gaussian Markov random field. One of the main advantages of this approach is the fact that GMRFs are defined by sparse matrices, allowing computationally effective methods.

In this paper we propose a spatio-temporal formulation of point processes with stochastic intensity, using a decomposition of the intensity function into components that vary in time and space. Specifically, we propose to use a LGCP structure, where the intensity function is decomposed into trend, seasonal, and cycle components together with spatial random effects, which allows us to identify permanent changes, and cyclical and seasonal effects. To perform inference procedure, we use the SPDE approach, allowing the use of Bayesian inference procedures based on INLA.

We first give a brief description of the SPDE approach, and a detailed discussion can be found in (Lindgren et al., 2011; Simpson et al., 2016). Spatio-temporal data can be represented as realizations of a stochastic process indexed by a space and a time dimension

$$Y(s,t) = \{y(s,t) | (s,t) \in D \times T \in \mathbb{R}^2 \times \mathbb{R}\} \tag{1}$$

where D is a subset of $\mathbb{R}^2$, T is a subset of $\mathbb{R}$, s denotes a spatial coordinate and t denotes a time index. Using this structure, we can represent a spatio-temporal LGCP modelled as

$$\begin{aligned} Y(s,t) &= Poisson(|e(s,t)|exp(\lambda(s,t)), \\ \lambda(s,t) &= z(s,t)\beta + \xi(s,t) \\ \xi(s,t) &= \Phi\xi(s,t-1) + \omega(s,t) \end{aligned} \tag{2}$$

where $Y(s,t)$ is the number of occurrences in a region s and in time t, $e(s,t)$ is the exposure offset for the region s, $z(s,t)$ is a set of covariates observed in the location s and period t, and $\xi(s,t)$ are the spatial random effects represented by the Gaussian process $\omega(s,t)$ continuously projected in space and given by

$$Cov(\omega(s,t)\omega_(s',t')) = \begin{cases} 0 & \text{if } t \neq t' \\ \sigma^2 C(h) & \text{if } t = t' \end{cases} \qquad \text{for } s \neq s' \tag{3}$$

where $C(h)$ is a covariance function of the Matérn class, which can be written as

$$C(h) = \frac{2^{1-\nu}}{\Gamma(\nu)}(\kappa||h||)^{\nu} K_{\nu}(\kappa||h||) \tag{4}$$

where $h = ||s - s'||$ is the Euclidean distance between locations s and s', $\kappa > 0$ is a spatial scale parameter, $\nu > 0$ is the smoothness parameter and K_{ν} is a modified Bessel function. The marginal variance σ^2 is defined by:

$$\sigma^2 = \frac{\Gamma(\nu)}{4\pi\kappa^{2\nu}\tau^2\Gamma(\nu + \frac{d}{2})} \tag{5}$$

where τ is a scaling parameter and d is the space dimension. Additionally, we adopt a parameterization in terms of $\log\tau$ and $\log\kappa$ for the covariance function (Lindgren et al., 2011):

$$\log\tau = \frac{1}{2}\log\left(\frac{\Gamma(\nu)}{\Gamma(\alpha)(4\pi)^{d/2}}\right) - \log\sigma - \nu\log\rho$$

$$\log\kappa = \frac{\log(8\nu)}{2} - \log\rho \tag{6}$$

where $\rho = \frac{(8\nu)^{1/2}}{\kappa}$. This representation is advantageous since, conditional on the value of ν, it is necessary to estimate only two parameters.

Considering a bounded region $\Omega \in \mathbb{R}^2$, it follows that the likelihood for an LGCP associated with data $Y = \{s_i \in \Omega : i = 1,\ldots,n; t = 1,\ldots,T\}$ is of the form

$$\pi(Y|\lambda) = \exp\left(|\Omega| - \int_\Omega \lambda(s,t)ds\right)\prod_{t=1}^{T}\prod_{i=1}^{n_t}\lambda(s_i,t). \tag{7}$$

Due to the doubly-stochastic property of the intensity function, the likelihood in (7) is analytically intractable. Since the term $\omega(s,t)$ corresponds to a GF with Matérn covariance, it is possible to use the SPDE approach to approximate the initial GF to a GMRF. The first main important result for the SPDE approach, is the fact that a GF x(s) with the Matérn covariance function is a stationary solution to the linear fractional SPDE (Whittle, 1954; Lindgren et al., 2011)

$$(\kappa - \Delta)^{\alpha/2}x(s) = W(s), \quad s \in \mathbb{R}^d, \quad \alpha = \nu + d/2, \quad \kappa > 0, \quad \nu > 0 \tag{8}$$

where $\Delta = \sum_{i=1}^{d}\frac{\partial^2}{\partial s_i^2}$ is the Laplacian operator and $W(s)$ is a spatial white noise. Therefore, to find a GMRF approximation of a GF, it is necessary to find the stochastic weak solution of a SPDE, which can be constructed through Finite Method Elements (FEM) (Lindgren et al., 2011). Thus, the approximation of SPDE solution is given by

$$\omega(s,t) \approx \tilde{\omega}(s,t) = \sum_{j=1}^{n} w_j\varphi_j(s,t) \tag{9}$$

where n is the number of vertices of the triangulation, $\{w_j\}_{j=1}^n$ are the weights with Gaussian distribution and $\{\varphi_j\}_{j=1}^n$ are the basis functions defined for each node on the mesh. In summary, the idea is to calculate the weights $\{w_j\}$, which determine the values of the field at the vertices, while the values inside the triangles are determined by linear interpolation (Lindgren et al., 2011). Here, the basis functions are chosen to be piecewise linear on each triangle:

$$\varphi_l(s,t) = \begin{cases} 1 & \text{at vertex } l \\ 0 & \text{elsewhere} \end{cases} \tag{10}$$

The stochastic weak solution of (8) is found by requiring

$$\{\langle\phi, (\kappa^2 - \Delta)^{\alpha/2}\omega\rangle\}_\Omega \overset{d}{=} \{\langle\phi, W\rangle\}_\Omega, \tag{11}$$

where $\{\phi_i(s), i = 1,\ldots,m\}$ are test functions and "$\overset{d}{=}$" denotes equality in distribution. Replacing (9) in (11) gives us

$$\{\langle\phi_i, (\kappa^2 - \Delta)^{\alpha/2}\varphi_j\rangle\}_\Omega \mathbf{w} \overset{d}{=} \{\langle\phi_i, W\rangle\}_\Omega, \tag{12}$$

for $i = 1,\ldots,m$, where m is the number of test functions. The finite dimensional solution is obtained by finding the distribution for the Gaussian weights in equation (9) that fulfils (12) for only a specific set of test functions, with $m = n$. When $\phi_k = (\kappa^2 = \Delta)^{1/2}\varphi_k$ for $\alpha = 1$ and $\phi_k = \varphi_k$ for $\alpha = 2$, these two

approximations are denoted the *least squares* and the *Galerkin* solution, respectively. Choosing $\alpha = 2$ and $\phi_k = \varphi_k$ yields

$$\left(\kappa^2\{\langle\varphi_i,\varphi_j\rangle\} + \{\langle\varphi_i,-\Delta\varphi_j\rangle\}\right)\mathbf{w} \stackrel{d}{=} \{\langle\varphi_i, W\rangle\}. \tag{13}$$

Define the $n \times n$ matrices, $\mathbf{C}$ and $\mathbf{G}$ as

$$\begin{aligned} C_{ij} &= \langle\varphi_i,\varphi_j\rangle \\ G_{ij} &= \langle\nabla\varphi_i,\nabla\varphi_j\rangle, \end{aligned} \tag{14}$$

then a weak solution to (8) is given by (9), where

$$(\kappa^2\mathbf{C} + \mathbf{G})\mathbf{w} \sim N(0,\mathbf{C}) \tag{15}$$

and the precision of the weights, $\mathbf{w}$, is

$$\mathbf{Q}_{\alpha=\mathbf{2}} = (\kappa^2\mathbf{C} + \mathbf{G})^T\mathbf{C}^{-\mathbf{1}}(\kappa^2\mathbf{C} + \mathbf{G}). \tag{16}$$

Although G_{ij} and C_{ij} are sparse matrices, $\mathbf{C}^{-1}$ is not sparse. The solution is to replace $C_{ij} = \langle\varphi_i,\varphi_j\rangle$ by the diagonal matrix $C_{ii} = \langle\varphi_i, 1\rangle$, that yields a Markov approximation. Therefore, $\mathbf{w}$ is a GMRF with precision matrix defined by (16).

Replacing the GF $\omega(s,t)$ by the GMRF approximation $\tilde{\omega}(s,t)$ in equation (2), and approximating the integral in (7) by a quadrature rule, results that the approximate likelihood consists of $(n + n_t)T$ independent Poisson random variables, where n is the number of vertices and n_t is the number of observed point processes. By obtaining the LGCP likelihood approximation, it is possible to perform inference procedures through the INLA algorithm, which provides accurate and efficient approximations on Bayesian hierarchical models that can be represented as latent Gaussian models. For reasons of space, we do not detail the INLA method here, which can be found in (Rue et al., 2009).

The dynamic formulation proposed in this paper is a generalization of the formulation given in Equation (2). In this case, we include the components μ_t, s_t and c_t as follows:

$$\begin{aligned} Y(s,t) &= Poisson(|e(s,t)|exp(\lambda(s,t)), \\ \lambda(s,t) &= \mu_t + s_t + c_t + z(s,t)\beta + \xi(s,t) \\ \mu_t &= \mu_{t-1} + \eta_\mu \\ s_t &= s_{t-1} + s_{t-2} + \ldots + s_{t-m} + \eta_s \\ c_t &= \theta_1 c_{t-1} + \theta_2 c_{t-2} + \eta_c \\ \xi(s,t) &= \Phi\xi(s,t-1) + \omega(s,t) \end{aligned} \tag{17}$$

where μ_t is the long term trend modeled as a first-order random walk (RW1), also known as the local-level model. This component is closely related to changes in the permanent patterns of fire occurrence in the Legal Amazon, and it can be seen as the accumulation of all shocks that occurred in the past with non-transitory effects. The s_t represents the seasonal components, which is based on a formulation of mean effects by period. The c_t is a cycle component represented by an second-order autoregressive process with possible complex roots, which allows to capture cyclic patterns if the roots are complex numbers (Laurini, 2019). The η_μ, η_c and η_s are nonspatial independent innovations with $\eta_\mu \sim N(0,\sigma^2_{\eta_\mu})$, $\eta_c \sim N(0,\sigma^2_{\eta_c})$ and $\eta_s \sim N(0,\sigma^2_{\eta_s})$. In all estimation procedures, we use default priors for the SPDE model in the R-INLA package implementation, which is available upon request from the authors.

3. Empirical Analysis. This section of the paper reports empirical analysis of the above method to the study of the changes in the patterns of fire occurrence in Legal Amazon between 2003 and 2020. The data sources are described below, before reporting the results of the proposed analysis.

3.1. *Data.* We use in this paper daily data of fire occurrence in the Legal Amazon from MODIS Thermal Anomalies/Fires between January 2003 and July 2020, which provides information such as fire occurrences (day/night), fire location, the logical criteria for the fire selection, and detection confidence. In order to provide better interpretations of the results, we use a quarterly aggregation of the daily data. In addition, from the computational aspect, the use of a very high frequency could lead to numerical problems in the estimation and inference processes since the dimension of the spatio-temporal covariance matrix is given by the Kronecker product between the time and spatial dimensions.

To illustrate, Figure 1 provides the number of fire events over time in the Legal Amazon, while Figure 2 shows a graphical distribution of the fires over time and space. From July to October 2005 large areas of the Amazon region experienced one of the most strong drought of the past 100 years (Marengo et al., 2008). The event in 2005 was driven by elevated tropical North Atlantic sea surface temperatures associated with a weaker cold anomaly in the South Atlantic (Marengo et al., 2008; Cox et al., 2008), and caused intense forest fire. After the peak in 2005, the fire occurrence in the Legal Amazon decreased until 2012, whereas from 2013 to 2020 forest fires increased (see Fig. 1). The spatial distribution of fire occurrence shows that forest fires are more concentrated in the region called "arc of deforestation", an area that extends from Maranhão to Acre, but with a pattern of increasing toward central areas. Additionally, it is possible to note that most of the fire events occur during the third and fourth quarter, the dry season (May to October).

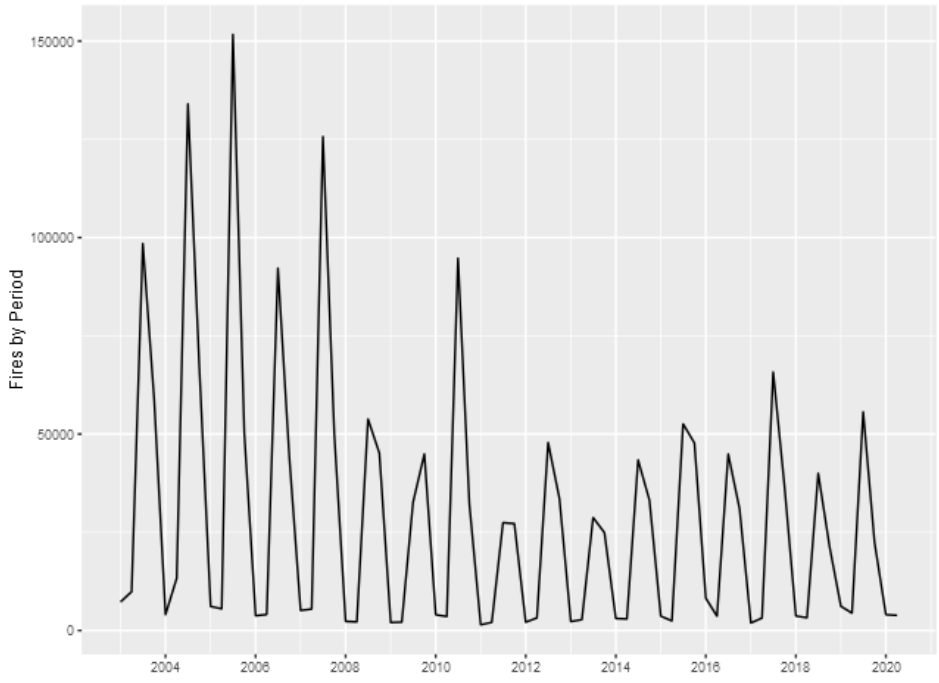

Fig 1: Fires in Legal Amazon by quarter between 2003 and 2020

Since our data base includes fire occurrence of different causes, such as human sources (deliberately or accidentally), and natural causes, it is important include explanatory variables in the analysis to control the main fixed effects related to climatic conditions and to control for possible use of the soil in agricultural activities. Thus, to explore the effects of climate change on fire patterns in the Legal Amazon, we include explanatory variables, such as MODIS Land Cover Classification, and Koppen Climate Classification system (Alvares et al., 2013). The MODIS land cover classification (see Appendix) uses the classification scheme defined by the International Geosphere-Biosphere Programme (IGBP) (Loveland and Belward, 1997), which includes 17 broad land cover and vegetation types. According to MODIS land cover, the Legal

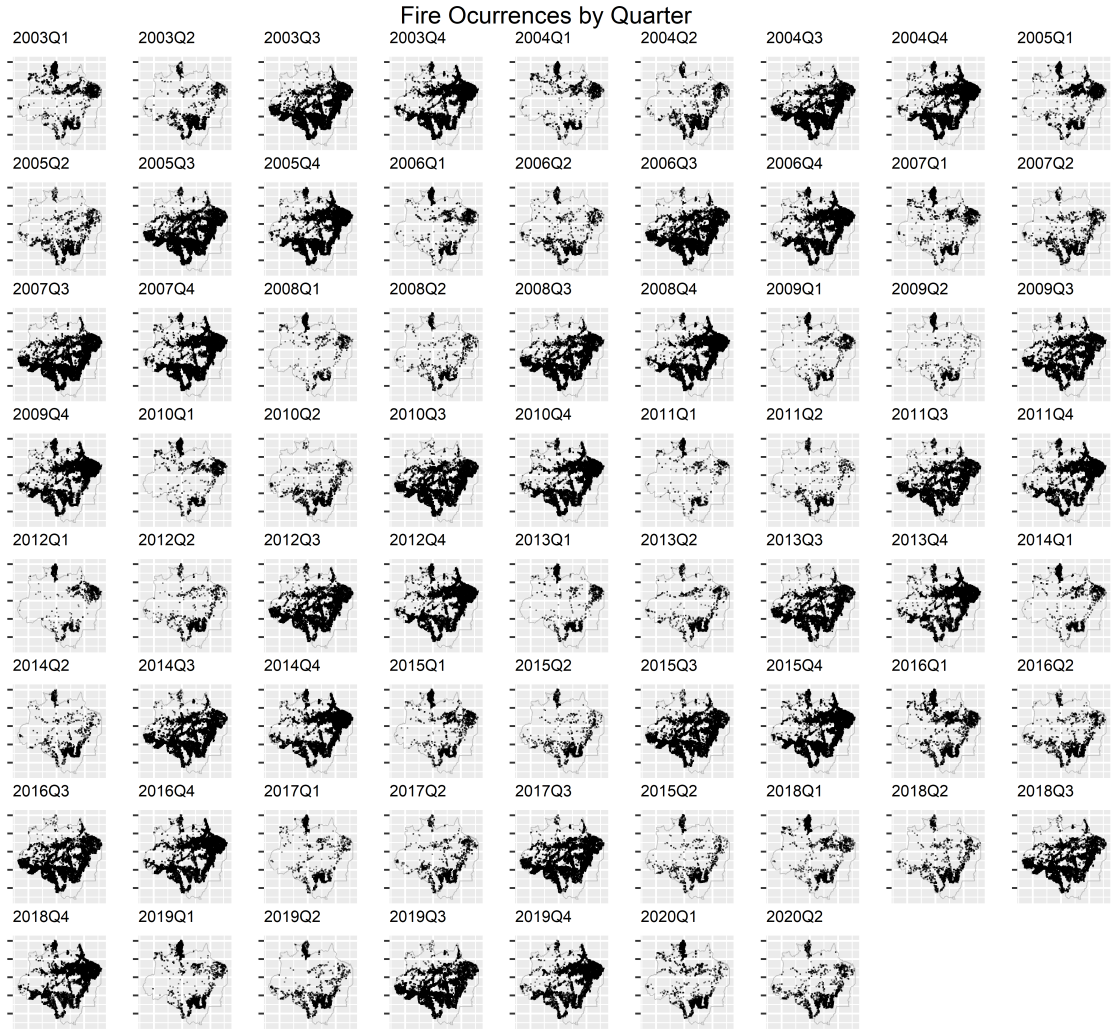

Fig 2: Spatial distribution of fires in Legal Amazon between 2003 and 2020

Amazon consists predominantly of tropical forest (evergreen broadleaf forests) but also of cerrado (shrubland and savannas, low tree cover), agriculture, and pasture land (cropland and cropland/natural vegetation mosaic). The Koppen climate types (see Appendix) are characterized by two or three characters, where the first indicate the climate zone defined by the temperature and rainfall, the second is defined by the rainfall distribution and the third considers the sea seasonal temperature variation (Alvares et al., 2013). According to Köppen Classification (Figure 2), the climate in the Legal Amazon is wet tropical (Am) in the central areas, tropical with dry winter (Aw) in the South Eastern Amazon and tropical without dry season (Af) in Western Amazon.

Evidence of intentional fire can be seen through the proximity of fire outbreaks and highways, as proximity to highways implies in human accessibility and lower transportation costs for agricultural production. Therefore, as explanatory variable, we also include the distance of fire occurrence from federal and state highways. The data base containing the location of federal and state highways is provided by *Departamento Nacional de Infraestrutura de Transportes* (DNIT) and *Empresa de Planejamento e Logística* (EPL).

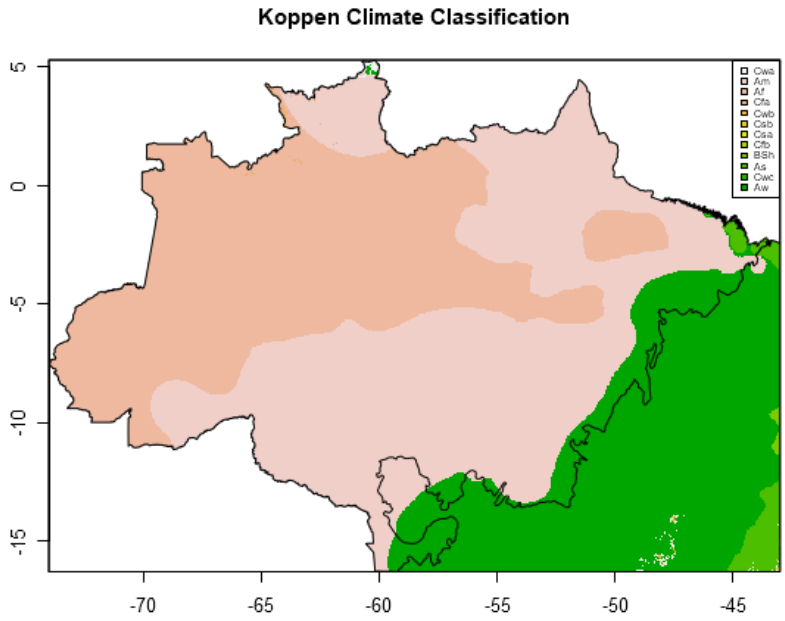

Fig 3: Köppen Climate Classification in Legal Amazon

3.2. *Results.* We perform inference procedure based on the the specification described in Equation (17). Thus, the estimated parameters are the precision of the trend component ($1/\eta_\mu$), seasonal component ($1/\eta_s$), and cycle component ($1/\eta_c$), the parameters of the second-order autoregressive process of the cycle (PACF1 and PACF2), the parameters associated with the set of observed covariates (β), the parameters of spatial covariance ($\log\tau$ and $\log\kappa$), and the parameter of spatial time dependence (Φ).

Table 1 reports the estimated parameters. As might be expected, the results indicate a negative relation between the distance to roads and the fire occurrence. The importance of the highways as a prime driver of fire occurrence and deforestation at local scales has been discussed in the literature, showing that the road plays an important role facilitating transformation of land-use practices, creating fresh access to new settlements in frontier regions, and reducing transportation costs in earlier settled areas (Ferraz, 2001; Fearnside, 2006).

As described earlier, the climate of the Legal Amazon, according to Köpper classification, are mostly wet climate, occurring precipitation in all months of the year (Af), monsoon, with a mean annual total precipitation $>$ 1500mm and a dry season occurring between August and November (Am), and tropical with dry season (Aw). As expected, obtained results suggest that the Am and Aw types of climate have higher influence on fire occurrence than Af type of climate. Furthermore, the results associated to land cover classifications show a positive relation between fire occurrence and savannas (S), woody savannas (WS), grasslands (G), and wetland ecosystems (PW). In these type of landscape, categorized as fire-dependent/influenced landscape, natural low-intensity fire regimes are mainly associated to the occurrences of lightening during wet season (Alves and Pérez-Cabello, 2017). On the other hand, the estimated parameters indicate a negative relation between fire occurrence and croplands (C), and urban and built-up lands (U). Although fire is widely used to convert natural forest into pastureland and cropland, the presence of cropland or pasture can reduce fire occurrence in the surrounding landscape by muting burned area (Archibald et al., 2009; Andela and Van Der Werf, 2014). Additionally, humans have manipulated fire regimes for several thousand years, suppressing wildfires to protect lives and properties, and creating landscapes that inhibit large-scale fire spread. As a consequence, such anthropogenic influences result in fire regimes that differ in terms of frequency, severity,

TABLE 1
Estimated Parameters

	Mean	SD	0.025quant	0.5quant	0.975quant	Mode
Fixed effects						
Distance Highways	-0.014	0.001	-0.016	-0.014	-0.011	-0.014
Köppen 1 (Cwa)	-0.386	0.255	-0.888	-0.386	0.114	-0.386
Köppen 2 (Am)	0.458	0.068	0.326	0.458	0.591	0.458
Köppen 3 (Af)	0.081	0.096	-0.107	0.081	0.268	0.081
Köppen 4 (Cfa)	-0.561	0.275	-1.102	-0.561	-0.024	-0.560
Köppen 10 (As)	-0.328	0.187	-0.696	-0.328	0.039	-0.328
Köppen 12 (Aw)	0.357	0.144	0.074	0.357	0.640	0.357
Land Cover 4 (DBF)	0.443	0.146	0.156	0.443	0.730	0.443
Land Cover 5 (MF)	-0.245	0.296	-0.827	-0.245	0.334	-0.245
Land Cover 8 (WS)	0.056	0.072	-0.085	0.056	0.197	0.056
Land Cover 9 (S)	0.111	0.057	-0.001	0.111	0.222	0.111
Land Cover 10 (G)	0.042	0.062	-0.079	0.042	0.163	0.042
Land Cover 11 (PW)	0.168	0.125	-0.078	0.168	0.414	0.168
Land Cover 12 (C)	-0.066	0.112	-0.286	-0.066	0.153	-0.066
Land Cover 13 (U)	-0.198	0.328	-0.842	-0.198	0.446	-0.197
Land Cover 17 (WB)	0.190	0.118	-0.042	0.190	0.422	0.191
Random Effects						
Precision for trend	75.270	9.664	55.629	75.786	92.789	78.179
Precision for seasonality	27.048	2.334	22.959	26.866	32.107	26.407
Precision for cycle	6.626	0.577	5.523	6.619	7.788	6.627
PACF1 for cycle	-0.366	0.140	-0.645	-0.353	-0.148	-0.241
PACF2 for cycle	0.147	0.055	0.038	0.148	0.252	0.151
Log τ	-2.139	0.013	-2.164	-2.139	-2.113	-2.139
Log κ	-0.105	0.013	-0.129	-0.105	-0.078	-0.107
Group Φ	0.859	0.005	0.847	0.859	0.868	0.860

Note: DBF: deciduous broadleaf forests. MF: mixed forests. WS: woody savannas. S: savannas. G: grasslands. PW: permanent wetlands. C: croplands. U: urban and built-up lands. WB: water bodies.

and seasonality from how ecosystems would burn in the absence of humans (Rabin et al., 2015; Syphard et al., 2017).

In relation to the random effects, the precision parameters represent the variability associated with the trend, seasonal and cycle components, where high values indicate low variability. Based on the results reported in the Table 1, it is possible to note a high precision associated with the seasonal component as well as the trend component, whereas the cycle component shows a relatively minor precision.

A primary empirical motivation for the present study was to assess the existence of changes in the patterns of fire occurrence in the Legal Amazon. To better understanding the results, we plotted the estimated trend, seasonal and cycle components (posterior mean and 95% Bayesian credibility interval; see Fig. 4). The trend component exhibit a relatively stable pattern, with a decrease between 2006 and 2012, which was brought about by a variety of factor, including governance measures and market mechanisms. First, decreases in agricultural output prices, and the availability of official rural credit may have contributed to changes in farmers' production decisions and thereby inhibiting the forest clearing for the expansion of farmland, reducing fire occurrences. While price increases provide incentive to expand the production, price decreases contribute to the opposite behavior and thereby reduce the deforestation, and consequently, decrease the fire occurrence. Similarly, official credit may be used to increase rural production, increasing fire occurrence by incorporating new lands for production, while credit constraints may lead to decreases in fire occurrence. Second, the set of policies adopted to reduce the deforested area underwent significant revisions during 2000s, introducing innovative procedures for monitoring, environmental control, and territorial management, such as the Action Plan for the Prevention and Control of Deforestation in the Legal Amazon (PPCDAm) launched in

2004. Additionally, novel policy measures were implemented in 2008, targeting municipalities with critical rates of deforestation and constraining rural credit (Assunção et al., 2015). The effectiveness of the policies and how the market mechanisms have impacted the deforestation in the Legal Amazon has been widely discussed in the literature, showing that, in general, the conservation policies, the decreases in agricultural prices, and the availability of rural credit has curbed deforestation (e.g., Assunçãoa et al. (2013); Hargrave and Kis-Katos (2013); Assunção et al. (2015)). Also, it is worth noting that, after 2012, the long-term component shows a pattern of growth, but without reaching the level of 2003. Furthermore, our model also captured important variations in the seasonal component, where it is possible to see a decrease in the range of seasonal fire occurrence, i.e., the fire occurrence has become more consistent throughout the year in the Legal Amazon, providing evidence of the increasing of fuel management practices occurring during the nonfire season, suggesting the expansion of agricultural production.

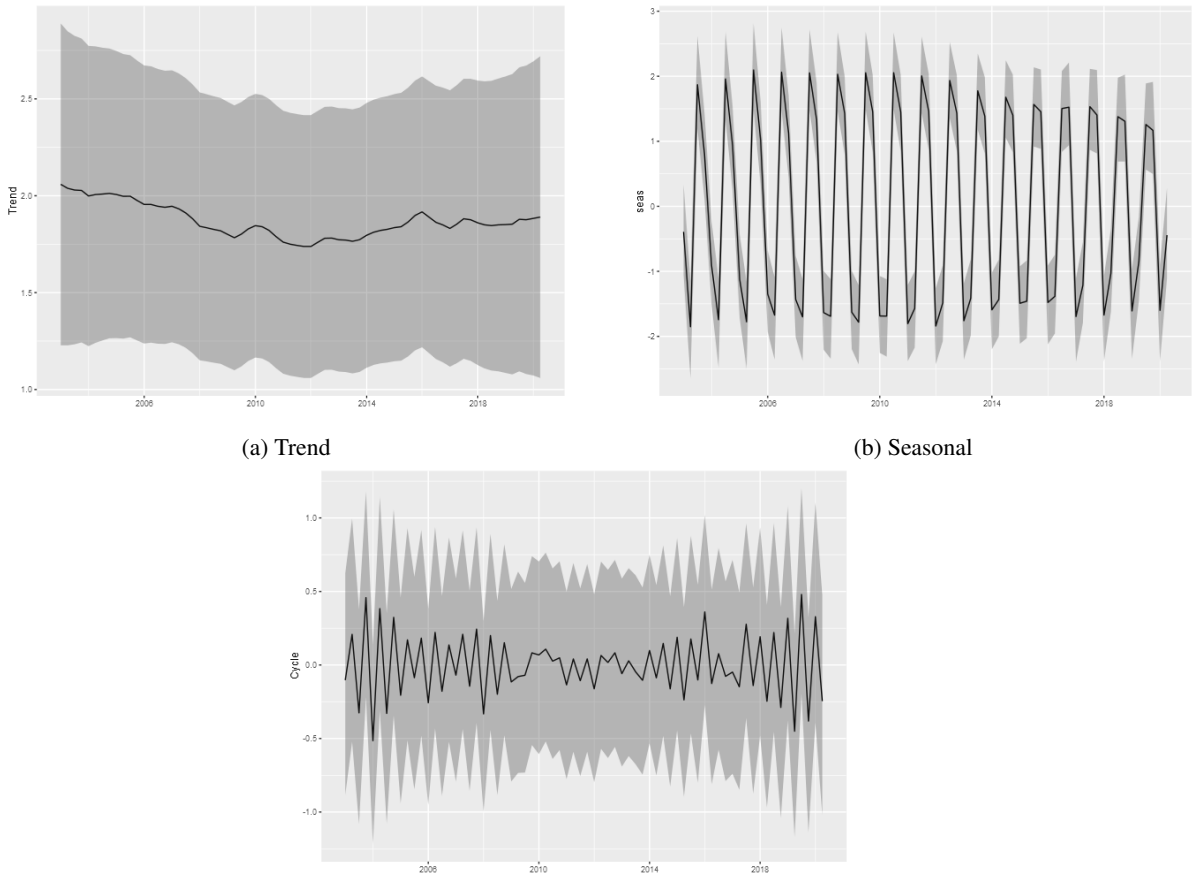

(a) Trend

(b) Seasonal

(c) Cycle

Fig 4: Trend, Seasonal and Cycle decomposition of fire occurrences in the Legal Amazon.

Additionally, it is possible to model the trend component as a second-order random walk (RW2), which imposes a smoothness structure that is able to identify the trend component. The RW2 structure can be thought as a non-parametric trend structure since it can be related to spline models (e.g. Green and Silverman (1994); Rue and Held (2005); Lindgren and Rue (2008)), which allows to identify the persistent patterns of long-term change. Therefore, in order to compare the results, we also performed inference procedure with the dependency structure in the trend component modelled as

$$\Delta^2 \mu_t = \mu_t - 2\,\mu_{t+1} + \mu_{t+2} \sim N(0, \sigma^2_{\eta_\mu}). \tag{18}$$

With the trend component modeled as RW2, the model was able to capture a growth pattern in the trend component between 2013 and 2016, and after 2018 (see Fig. 5). It is worth noting that the increasing of fire occurrence have trended upward since 2013, reaching a peak in 2016. Along with population growth, investment, and new roads, more international markets were opening for Brazilian beef during this period, increasing the pressure on forests. More importantly, the Brazil's Forest Code (Law 4771/1965) was replaced by Law 12651/2012, reducing restrictions and pardoning areas of illegal clearing done by 2008, causing significant environmental and social issues (Fearnside, 2017). Aggravating the situation was the political uncertainty and the atypical activities surrounding Dilma Rousseff's impeachment proceeding in 2016, which offered an opportunity to approve legislative initiatives to remove environmental restrictions (Fearnside, 2016). Furthermore, market conditions may have contributed to the increase in the fire occurrence in 2016, such as the low value of the Brazilian real relative to the US dollar, increasing the exportation of soy and beef (Fearnside, 2017).

Also, our proposed model captured the increasing of fire occurrences after 2018, which may be linked to the recent Brazilian environmental policies adopted by former President Michel Temer and also by the current president, Jair Bolsonaro. Michel Temer assumed Brazilian presidency in June 2016, supported by conservative politicians linked to the production of agricultural commodities or financed by agribusiness groups. The measures approved by Temer including the PEC 65, which eliminated the need for environmental licensing for construction and stimulated the constructions of highways and dams in the Amazon region, potentially increasing deforestation rates. Also, the government established a cap for public spending growth over 20-year period (PEC 241), affecting the Ministry of Environment, which is responsible for important national institutes that directly control the Amazon regions, such as the Brazilian Institute of Environment and Renewable Natural Resources (IBAMA) and the Chico Mendes Institute for Biodiversity Conservation (ICMBio) (Pereira et al., 2019). Similarly, Jair Bolsonaro, which have assumed Brazilian presidency in 2019 and, in exchange for political support of the ruralist group, he introduced several measures that encourage the expansion of agriculture and livestock, such as drastic reduction in funds for controlling and monitoring Amazon forest and freer use of agrochemicals and pesticides, leads to substantial environmental damage (Pereira et al., 2020).

The spatial heterogeneity of the fire occurrence in the Legal Amazon can be seen through the estimated spatial random effect, where the trend component was modeled as RW2 (posterior mean of estimated spatial random effect; see Fig. 6). It is possible to observe that the spatial random effects capture the variability in the Legal Amazon, especially in the regions classified as wet tropical (Am), which is characterized by a dry season, that occurs between August and November (third and fourth quarters), and tropical with dry season (Aw). On the other hand, in western Amazon, where the climate is predominantly tropical without dry season (Af), the variability is low. Additionally, to show the model's ability to fit the fire occurrence, we plotted the estimated log intensity function and the observed fire occurrence (black dots; see Fig. 7), which shows that the estimated log intensity function explains the spatio-temporal variation observed in the fire count in the Legal Amazon, suggesting that the model has a good fit.

4. Conclusion. The Amazon biome plays an important role in the climate system, with relevance at regional and global scales. Fire occurrences, related to both natural and anthropogenic activities, are relevant disturbances in the Legal Amazon, with significant effects. Changes in the patterns of fire occurrence in the Amazon region have been widely reported in the literature and are related with a variety of factors, including dry conditions, deforestation, agricultural expansion, climate changes, and climatic anomalies such as El Ninõ events.

The purpose of this paper was to analyze the existence of changes in the patterns of the fire occurrence in the Legal Amazon, within the spatio-temporal point process framework. To perform inference procedures, we proposed a structural decomposition to spatio-temporal point pattern data. In particular, we proposed to use a dynamic representation of a Log Gaussian Cox process where the intensity function was modeled through the decomposition of components into trend, seasonality, cycles, covariates and spatial effects. This useful formulation was able to capture permanent changes in the fire occurrence and also, to identify seasonal

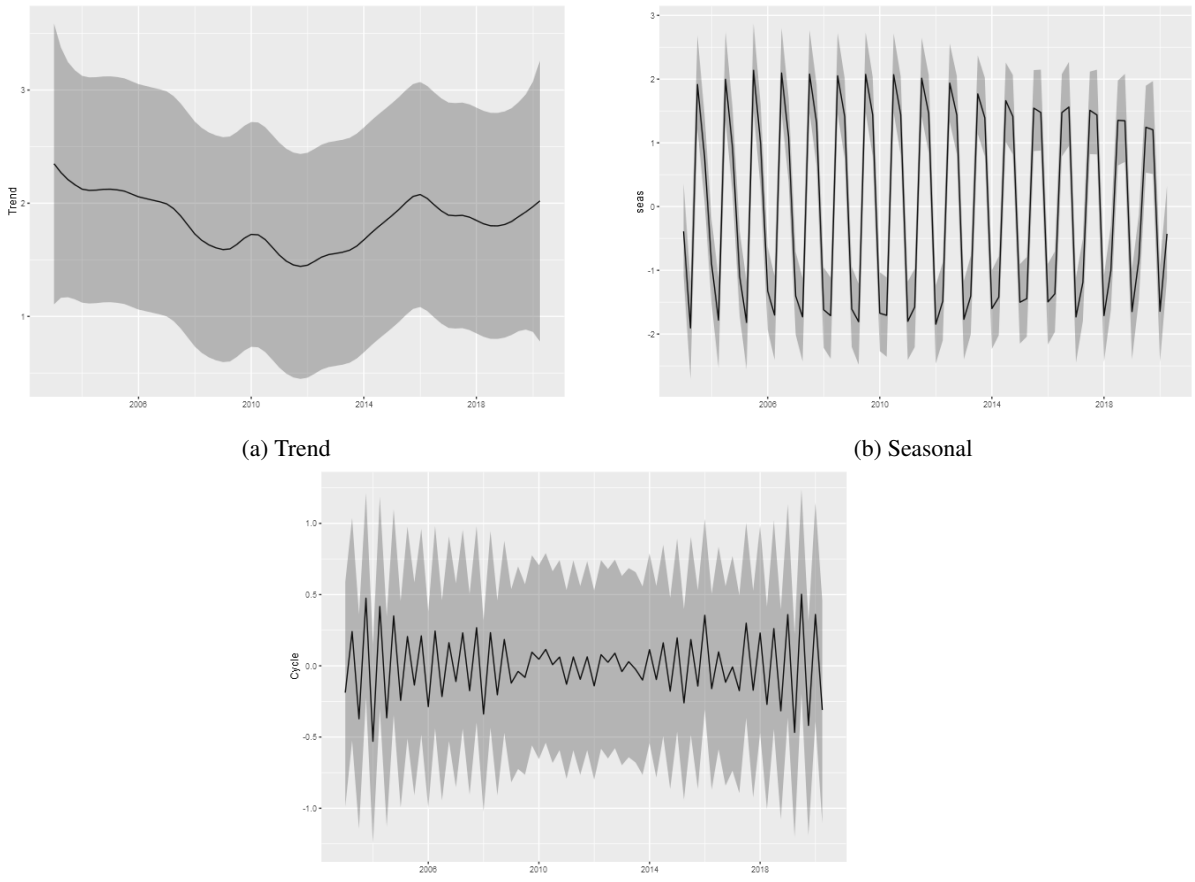

(a) Trend

(b) Seasonal

(c) Cycle

Fig 5: Trend, Seasonal and Cycle decomposition of fire occurrences in the Legal Amazon - RW2

and cyclic effects. Plus, the resulting Bayesian hierarchical structure allowed us to perform inference in a computationally effective way within the integrated nested Laplace approximation framework.

We presented here, the results of analyzing data for fire occurrence in the Legal Amazon reported by MODIS, from January 2003 to February 2020. Also, we included explanatory variables to control the main fixed effect related to climatic conditions and the use of the soil in agricultural activities. Our results showed that long-term movements of fire occurrence dropped considerably between 2006 and 2012, which suggest that conservation regulations and/or market conditions in the mid-2000s were effective in reducing the deforestation rates and, consequently, decreasing the fire occurrence. Also, our model captured an increase in the trend component between 2013 and 2016, and after 2018, which maybe explained by localized drivers, such as population growth, investments, and roads, associated with political measures that encourage the expansion of agriculture and livestock. Furthermore, variations in the estimated seasonal component provided evidence that the fire occurrence has become more consistent throughout the year, suggesting the increase of fuel management practices occurring during the nonfire season, which is related to the expansion of agricultural production.

REFERENCES

Alvares, C.A., Stape, J.L., Sentelhas, P.C., de Moraes, G., Leonardo, J., Sparovek, G., 2013. Köppen's climate classification map for brazil. Meteorologische Zeitschrift 22, 711–728.

Alves, D.B., Pérez-Cabello, F., 2017. Multiple remote sensing data sources to assess spatio-temporal patterns of fire incidence over campos Amazônicos savanna vegetation enclave (Brazilian Amazon). Science of The Total Environment 601, 142–158.

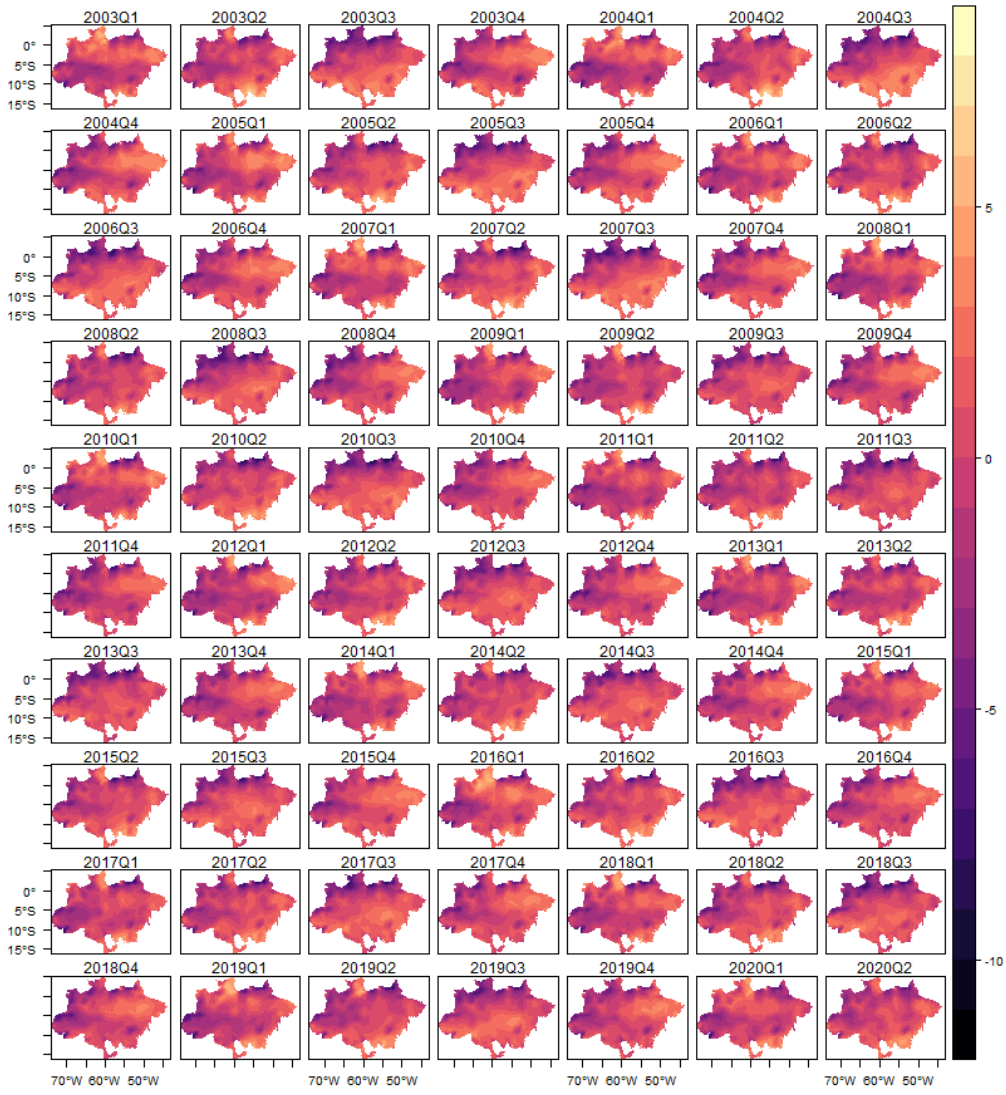

Fig 6: Spatial Random Effects.

Andela, N., Van Der Werf, G.R., 2014. Recent trends in african fires driven by cropland expansion and El Nino to La Nina transition. Nature Climate Change 4, 791–795.

Aragão, L.E.O., Malhi, Y., Roman-Cuesta, R.M., Saatchi, S., Anderson, L.O., Shimabukuro, Y.E., 2007. Spatial patterns and fire response of recent Amazonian droughts. Geophysical Research Letters 34.

Archibald, S., Roy, D.P., van Wilgen, B.W., Scholes, R.J., 2009. What limits fire? an examination of drivers of burnt area in Southern Africa. Global Change Biology 15, 613–630.

Assunção, J., Gandour, C., Rocha, R., et al., 2015. Deforestation slowdown in the Brazilian Amazon: prices or policies. Environment and Development Economics 20, 697–722.

Assunçãoa, J., Gandoura, C., Rochaa, R., Rochab, R., 2013. Does credit affect deforestation? evidence from a rural credit policy in the Brazilian Amazon. Climate Policy Initiative, Rio de Janeiro, Brasil .

Bloomfield, P., 1992. Trends in global temperature. Climatic Change 21, 1–16.

Cochrane, M.A., Alencar, A., Schulze, M.D., Souza, C.M., Nepstad, D.C., Lefebvre, P., Davidson, E.A., 1999. Positive feedbacks in the fire dynamic of closed canopy tropical forests. Science 284, 1832–1835.

Cochrane, M.A., Barber, C.P., 2009. Climate change, human land use and future fires in the Amazon. Global Change Biology 15, 601–612.

Cochrane, M.A., Schulze, M.D., 1999. Fire as a recurrent event in tropical forests of the eastern Amazon: Effects on forest structure, biomass, and species composition 1. Biotropica 31, 2–16.

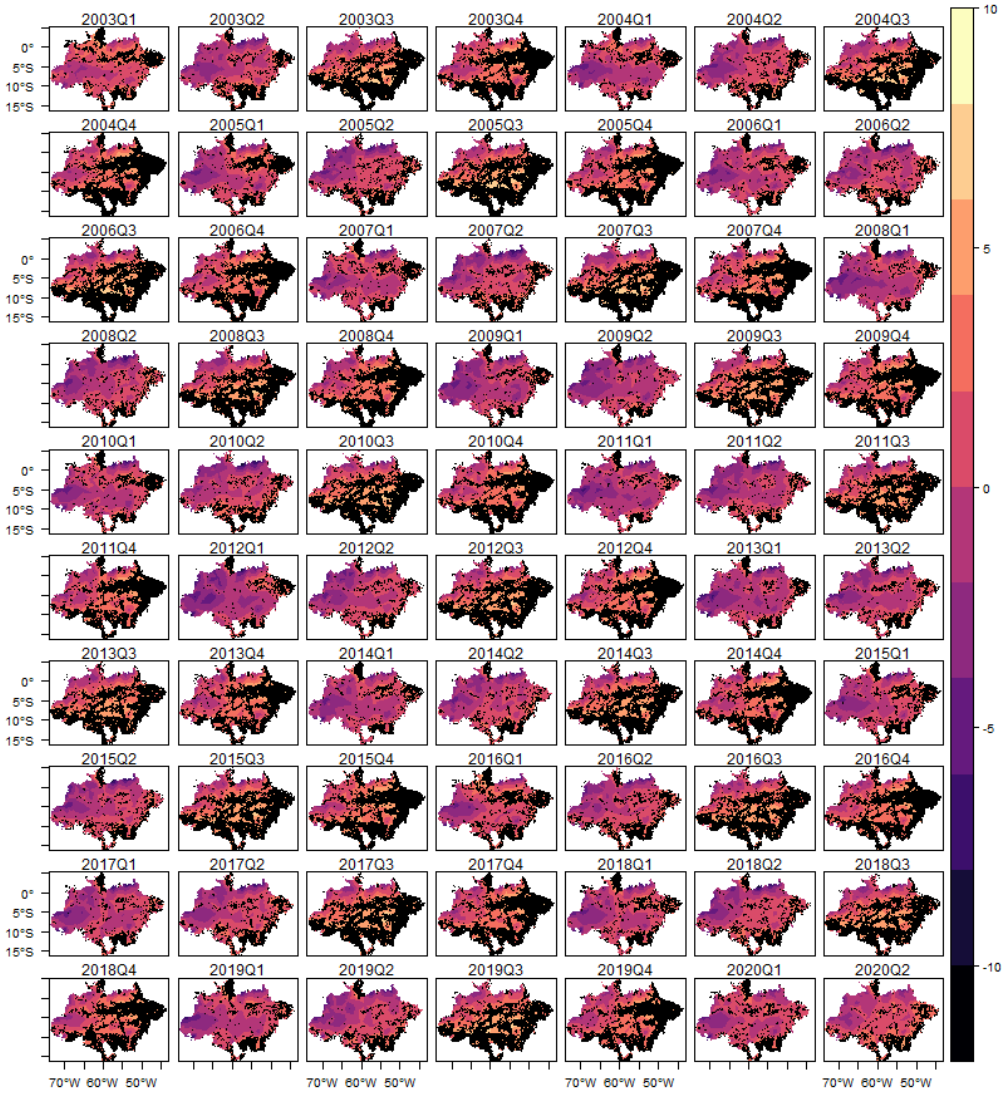

Fig 7: Estimated log-internsity function and observed fire occurrence.

Costa, M.H., Yanagi, S.N., Souza, P.J., Ribeiro, A., Rocha, E.J., 2007. Climate change in Amazonia caused by soybean cropland expansion, as compared to caused by pastureland expansion. Geophysical Research Letters 34.

Cox, P.M., Harris, P.P., Huntingford, C., Betts, R.A., Collins, M., Jones, C.D., Jupp, T.E., Marengo, J.A., Nobre, C.A., 2008. Increasing risk of Amazonian drought due to decreasing aerosol pollution. Nature 453, 212–215.

Crutzen, P.J., Andreae, M.O., 1990. Biomass burning in the tropics: Impact on atmospheric chemistry and biogeochemical cycles. Science 250, 1669–1678.

De Mendonça, M.J.C., Diaz, M.d.C.V., Nepstad, D., da Motta, R.S., Alencar, A., Gomes, J.C., Ortiz, R.A., 2004. The economic cost of the use of fire in the Amazon. Ecological Economics 49, 89–105.

De Mendonça, M.J.C., Sachsida, A., Loureiro, P.R., 2006. Estimation of damage to human health due to forest burning in the Amazon. Journal of Population Economics 19, 593–610.

Fearnside, P., 2017. Deforestation of the Brazilian Amazon, in: Oxford Research Encyclopedia of Environmental Science.

Fearnside, P.F., 2006. Containing destruction from Brazil's amazon highways: now is the time to give weight to the environment in decision-making. Environmental Conservation 33, 181–183.

Fearnside, P.M., 2012. Brazil's Amazon forest in mitigating global warming: unresolved controversies. Climate Policy 12, 70–81.

Fearnside, P.M., 2016. Brazilian politics threaten environmental policies. Science 353, 746–748.

Ferraz, C., 2001. Explaining agriculture expansion and deforestation: evidence from the Brazilian Amazon-1980/98 .

Food, of The United Nations, A.O., 2020. State of the World's Forests.

Gedney, N., Valdes, P.J., 2000. The effect of Amazonian deforestation on the northern hemisphere circulation and climate. Geophysical Research Letters 27, 3053–3056.

Green, P., Silverman, B., 1994. Nonparametric Regression and Generalized Linear Models: A Roughness Penalty Approach. CRC Press.

Hargrave, J., Kis-Katos, K., 2013. Economic causes of deforestation in the Brazilian Amazon: a panel data analysis for the 2000s. Environmental and Resource Economics 54, 471–494.

Illian, J., Sørbye, S., Rue, H., Hendrichsen, D., 2010. Fitting a log Gaussian Cox process with temporally varying effects–a case study. Preprint Statistics .

Laurini, M., 2019. A spatio-temporal approach to estimate patterns of climate change. Environmetrics 30, e2542.

Li, W., Fu, R., Dickinson, R.E., 2006. Rainfall and its seasonality over the Amazon in the 21st century as assessed by the coupled models for the IPCC AR4. Journal of Geophysical Research: Atmospheres 111.

Lindgren, F., Rue, H., 2008. On the second-order random walk model for irregular locations. Scandinavian Journal of Statistics 35, 691–700.

Lindgren, F., Rue, H., Lindström, J., 2011. An explicit link between Gaussian fields and Gaussian Markov random fields: the stochastic partial differential equation approach. Journal of the Royal Statistical Society: Series B (Statistical Methodology) 73, 423–498.

Longo, K., Freitas, S., Andreae, M., Yokelson, R., Artaxo, P., 2009. Biomass burning in Amazonia: Emissions, long-range transport of smoke and its regional and remote impacts. Geophysical Monograph Series 186, 207–232.

Loveland, T.R., Belward, A., 1997. The igbp-dis global 1km land cover data set, DISCover: first results. International Journal of Remote Sensing 18, 3289–3295.

Malhi, Y., Roberts, J.T., Betts, R.A., Killeen, T.J., Li, W., Nobre, C.A., 2008. Climate change, deforestation, and the fate of the Amazon. science 319, 169–172.

Marengo, J.A., 2004. Interdecadal variability and trends of rainfall across the Amazon basin. Theoretical and Applied Climatology 78, 79–96.

Marengo, J.A., Nobre, C.A., Tomasella, J., Oyama, M.D., Sampaio de Oliveira, G., De Oliveira, R., Camargo, H., Alves, L.M., Brown, I.F., 2008. The drought of Amazonia in 2005. Journal of Climate 21, 495–516.

Morton, D., Defries, R., Randerson, J., Giglio, L., Schroeder, W., Van Der Werf, G., 2008. Agricultural intensification increases deforestation fire activity in Amazonia. Global Change Biology 14, 2262–2275.

Morton, D.C., DeFries, R.S., Shimabukuro, Y.E., Anderson, L.O., Arai, E., del Bon Espirito-Santo, F., Freitas, R., Morisette, J., 2006. Cropland expansion changes deforestation dynamics in the southern Brazilian Amazon. Proceedings of the National Academy of Sciences 103, 14637–14641.

Nepstad, D., Lefebvre, P., Lopes da Silva, U., Tomasella, J., Schlesinger, P., Solórzano, L., Moutinho, P., Ray, D., Guerreira Benito, J., 2004. Amazon drought and its implications for forest flammability and tree growth: A basin-wide analysis. Global Change Biology 10, 704–717.

Nobre, C.A., Sellers, P.J., Shukla, J., 1991. Amazonian deforestation and regional climate change. Journal of Climate 4, 957–988.

Pereira, E.J.d.A.L., Ferreira, P.J.S., de Santana Ribeiro, L.C., Carvalho, T.S., de Barros Pereira, H.B., 2019. Policy in brazil (2016–2019) threaten conservation of the Amazon rainforest. Environmental Science & Policy 100, 8–12.

Pereira, E.J.d.A.L., de Santana Ribeiro, L.C., da Silva Freitas, L.F., de Barros Pereira, H.B., 2020. Brazilian policy and agribusiness damage the Amazon rainforest. Land Use Policy 92, 104491.

Proietti, T., Hillebrand, E., 2017. Seasonal changes in central England temperatures. Journal of the Royal Statistical Society: Series A (Statistics in Society) 180, 769–791.

Rabin, S.S., Magi, B., Shevliakova, E., Pacala, S.W., 2015. Quantifying regional, time-varying effects of cropland and pasture on vegetation fire. Biogeosciences 12, 6591–6604.

Rue, H., Held, L., 2005. Gaussian Markov Random Fields: Theory and Applications. CRC Press.

Rue, H., Martino, S., Chopin, N., 2009. Approximate bayesian inference for latent Gaussian models by using integrated nested Laplace approximations. Journal of the Royal Statistical Society: Series B (Statistical Methodology) 71, 319–392.

Serra, L., Saez, M., Mateu, J., Varga, D., Juan, P., Díaz-Ávalos, C., Rue, H., 2014. Spatio-temporal log-Gaussian Cox processes for modelling wildfire occurrence: the case of Catalonia, 1994–2008. Environmental and Ecological Statistics 21, 531–563.

Siegert, F., Ruecker, G., Hinrichs, A., Hoffmann, A., 2001. Increased damage from fires in logged forests during droughts caused by El Nino. Nature 414, 437–440.

Simpson, D., Illian, J.B., Lindgren, F., Sørbye, S.H., Rue, H., 2016. Going off grid: Computationally efficient inference for log-Gaussian Cox processes. Biometrika 103, 49–70.

Sulla-Menashe, D., Friedl, M.A., 2018. User guide to collection 6 MODIS land cover (MCD12Q1 and MCD12C1) product. USGS: Reston, VA, USA , 1–18.

Syphard, A.D., Keeley, J.E., Pfaff, A.H., Ferschweiler, K., 2017. Human presence diminishes the importance of climate in driving fire activity across the United States. Proceedings of the National Academy of Sciences 114, 13750–13755.

Teng, M., Nathoo, F., Johnson, T.D., 2017. Bayesian computation for log-Gaussian Cox processes: A comparative analysis of methods. Journal of Statistical Computation and Simulation 87, 2227–2252.

Valente, F., Laurini, M., 2020. Tornado occurrences in the united states: A spatio-temporal point process approach. Econometrics 8, 25.

Werth, D., Avissar, R., 2002. The local and global effects of Amazon deforestation. Journal of Geophysical Research: Atmospheres 107, LBA–55.
Whittle, P., 1954. On stationary processes in the plane. Biometrika , 434–449.

APPENDIX: LAND COVER AND CLIMATE CLASSIFICATION

TABLE 2
Köppen Climate Classification (Alvares et al., 2013)

Characters	**Description**
Cwa	(C) Humid subtropical (w) With dry winter (a) and hot summer.
Am	(A) Tropical (m) monsoon.
Af	(A) Tropical (f) without dry season.
Cfa	(C) Humid subtropical (f) Oceanic climate, without dry season (a) and hot summer.
Cwb	(C) Humid subtropical (w) With dry winter (b) and temperate summer.
Csb	(C) Humid subtropical (s) With dry summer (b) and temperate summer.
Csa	(C) Humid subtropical (s) With dry summer (a) and hot summer.
Cfb	(C) Humid subtropical (f) Oceanic climate, without dry season (b) and temperate summer.
BSh	(B) Dry (S) Semi-arid (h) low latitude and altitude.
As	(A) Tropical (s) with dry summer.
Cwc	(C) Humid subtropical (w) With dry winter and (c) short and cool summer.
Aw	(A) Tropical (w) with dry winter.

TABLE 3
MODIS land cover classification legend and class descriptions (Sulla-Menashe and Friedl, 2018)

Name	**Value**	**Description**
Evergreen Needleleaf Forests	1	Dominated by evergreen conifer trees (canopy>2m). Tree cover >60%
Evergreen Broadleaf Forests	2	Dominated by evergreen broadleaf and palmate trees (canopy>2m). Tree cover >60%
Deciduous Needleleaf Forests	3	Dominated by decidous needleaf (larch) trees (canopy >2m). Tree cover >60%
Deciduous Broadleaf Forests	4	Dominated by decidous broadleaf trees (canopy >2m). Tree cover >60%
Mixed Forests	5	Dominated by neither decidous nor evergreen (40-60% of each) tree type (canopy >2m). Tree cover >60%
Closed Shrublands	6	Dominated by woody perennials (1-2m height) >60% cover
Open Shrublands	7	Dominated by woody perennials (1-2m height) 10-60% cover
Woody Savannas	8	Tree cover 30-60% (canopy >2m)
Savannas	9	Tree cover 10-30% (canopy >2m)
Grasslands	10	Dominated by herbaceous annuals (<2m)
Permanent Wetlands	11	Permanently inundated lands with 30-60% water cover and >10% vegetated cover
Croplands	12	At leastt 60% of area is cultivated cropland
Urban and Built-up Lands	13	At least 30% impervious surface area including building materials, asphalt, and vehicles.
Cropland/Natural Vegetation Mosaics	14	Mosaics of small-scale cultivation 40-60% with natural tree, shrub, or herbaceous vegetation
Permanent Snow and Ice	15	At least 60% of area is covered by snow and ice for at least 10 months of the year
Barren	16	At least 60% of area is non-vegetated barren (sand, rock, soil) areas with less than 10% vegetation
Water Bodies	17	At least 60% of area is covered by permanent water bodies
Unclassified	255	Has not received a map label because of missing inputs